

Dislocation reduction in heteroepitaxial $\text{In}_x\text{Ga}_{1-x}\text{N}$ using step-graded interlayer for future solar cells

Md. Arafat Hossain · Md. Rafiqul Islam ·
M. K. Hossain · A. Hashimoto · A. Yamamoto

Received: 25 August 2013 / Accepted: 15 November 2013 / Published online: 7 December 2013
© The Author(s) 2013. This article is published with open access at Springerlink.com

Abstract The efforts on dislocation reduction have become a potential issue to realize the future high-efficiency solar cells using the InGaN materials. In this work, first, a numerical simulation has been carried out for the reduction of dislocation density in wurtzite InGaN heteroepitaxy using step-graded interlayers. An energy balance model has been developed for evaluating the misfit dislocation (MD) density. The residual strain from previous interlayer has been taken into account with misfit strain in each interlayer. A reaction model for threading dislocations (TDs) has also been developed and solved numerically considering the geometrical parameters. The simulation results confirmed a significant improvement of epilayer quality due to the use of step-graded interlayers. The calculations have been done for $1.5\ \mu\text{m}$ InGaN using 3 step-graded interlayers each containing 10 % composition difference and $0.2\ \mu\text{m}$ thickness. The edge, screw, and mixed type MDs are found to be 4.69×10^{10} , 4.53×10^9 , and $4.03 \times 10^{11}\ \text{cm}^{-2}$, respectively, on the $1/3 < 11\text{--}23 > (11\text{--}22)$ slip and similarly evaluated in other possible slips of the $\text{In}_{0.4}\text{Ga}_{0.6}\text{N}$. Significant decreases in MD densities have been evaluated for increasing interlayer up to 4 with 8 % In composition difference. The edge, screw, and

mixed MDs are found to be decreased from 3.25×10^{11} to 4.45×10^{10} , 3.2×10^{10} to 3.95×10^9 and 2.8×10^{12} to $1.77 \times 10^{11}\ \text{cm}^{-2}$ in $1/3 < 11\text{--}23 > (11\text{--}22)$ slip system using four interlayers. Besides, a higher rate of reduction has been reported for the step-graded structure especially for mixed type due to more relative motion and step inclination at each interlayer. The average edge, screw, and mixed type TD densities are found to be 1.48×10^{10} , 3.7×10^{10} , and $1.1 \times 10^9\ \text{cm}^{-2}$, respectively, at the top surface of the $\text{In}_{0.4}\text{Ga}_{0.6}\text{N}$ epilayer. Finally, experimental work has been done to realize the strain profile using reciprocal space mapping as well as dislocations considering the same films to compare the results. The outcome of the numerical simulation found good agreement with the experimental works as well as with the published experimental results.

Keywords InGaN · Critical thickness · Misfit dislocation · Threading dislocation · Interlayer

Introduction

In the recent years, group III-nitrides and their related alloys have been intensively studied with remarkable breakthrough in the growth of multilayer structures for device applications [1–3]. Among them the ternary alloy InGaN is currently a major topic of research in the field of the modern optoelectronic and microelectronic technologies [4, 5]. Especially, this material is a promising candidate for multi-junction tandem solar cells with high conversion efficiency [6–8]. In order to realize such solar cell, it is essential to grow this alloy with high indium (In) content [6]. As there is no successful technique devised for the bulk growth of InGaN they are usually grown

Md. A. Hossain · Md. R. Islam (✉)
Department of Electrical and Electronic Engineering, Khulna
University of Engineering and Technology, Khulna, Bangladesh
e-mail: rafiq043@yahoo.com

M. K. Hossain
Center of Research Excellence in Renewable Energy, King Fahd
University of Petroleum and Minerals (KFUPM), Dhahran
31261, Kingdom of Saudi Arabia

A. Hashimoto · A. Yamamoto
Graduate School of Engineering, University of Fukui, Fukui,
Japan

heteroepitaxially on GaN template [9]. Therefore, a large lattice (11 % between InN and GaN) as well as thermal expansion coefficient mismatches between the layer and substrate, introduces dislocations which lead to the degradation of the quality of this material and consequently the performance of its constituent devices [10–12]. These dislocations act as scattering centres and midband gap states, which proceed as recombination centres and reduce the minority carrier lifetime [13–15]. As a result, open-circuit voltage (V_{oc}), short-circuit current density (J_{sc}), fill factor, and efficiency of solar cells decrease gradually with the increase of dislocation density [13]. Hence the reduction of dislocation density is a budding issue for InGaN-based solar cells.

The concept of dislocation reduction during the heteroepitaxial growth of InGaN requires an understanding of misfit strain caused by lattice mismatch. Various theoretical as well as experimental evidences confirmed the common mode of strain relaxation as the formation of misfit dislocations (MDs) from different sources [11, 16–18]. The threading dislocations (TDs) which threaded the multilayer may be initiated from MDs or any other sources [16]. Other sources of dislocation such as V-defects and surface inclusions are also reported for single-phase high In-content InGaN on GaN [19]. Due to the adverse effects of dislocations, the researchers are highly interested to find a suitable growth technique which will reduce the dislocations density of future high-performance device fabrication. With this purpose, several efforts have been made to reduce MDs as well as TDs [20]. Ee et al. [21, 22] reported the nano-patterned AGOG (Deposition of Aluminum, Growth of Oxide, and Grain growth) sapphire for the growth of GaN template with reduced TD density in LEDs to enhance the output power. Compositional grading is one of the most effective techniques which can be very effective to reduce both MDs and TDs [23–28]. In a properly designed graded layer, misfit strain as well as dislocation is greatly reduced due to spreading the strain profile throughout the entire layer of thickness instead being concentrated to a single interface. This grading of epitaxial layer may be done in several approaches such as linear or nonlinear grading, step-grading, grading with overshoot interfaces, and reverse grading [23–28]. Most of the experimental and theoretical studies with graded heteroepitaxial layer have been carried out on linear and nonlinear grading [25, 29, 30]. However, the efficient strategy to reduce dislocation density is to initiate annihilation and fusion reaction among them during their glide process. In this process, the inclinations of TDs at layer-substrate or layer-layer interface are responsible for interaction between them and hence result in reduction by reaction [31]. Another approach for TD reduction is the incorporation of Si into the $Al_xGa_{1-x}N$ film that results in a proportional stress transition from compressive to tensile.

This dislocation reduction by Si doping also results from the increased TD inclination [32, 33]. Accordingly, linear or nonlinear grading shows poor performance for reducing the TDs in the epilayer due to the less interaction probability.

These objections are a driving force for further investigations of a technique which is best suitable for MDs as well as TDs reduction. In heteroepitaxy growth of InGaN using step-graded interlayer, due to the step increase of In composition in the epitaxial layers, a multiple step inclination of TDs at each interface will occur. This promotes the reaction among the TDs at each interlayer. Few experimental works on different material systems confirmed that this technology will be a promising solution for dislocation reduction during growth of heteroepitaxy [23, 24, 34–36]. Furthermore, the step-wise increase of In-content provides the facility to use of ternary InGaN as a substrate materials for the upper layers with high In-content. As a result, the reduced compressive strain between two successive layers improves the spontaneous emission properties and optical gain with reduced wavelength shift of multiple quantum well (MQW) devices [37–40]. Although available theoretical works have been developed for without grading or linear and nonlinear grading, there is no such work on step-graded interlayers for wurtzite materials. In order to realize future high-performance devices, a detailed analysis of dislocation reduction using step-graded interlayer and further optimization is urgently required.

In this work, an analytical energy balance model for MDs and reaction model for TDs has been developed for the optimized step-graded structure for the fabrication of future solar cells. The reaction model considered possible annihilation and fusion reaction between TDs and TD blocking by MDs. In addition, experimental works have been done according to the modeling and the observed results illustrated. Finally, the results obtained from these simulations have been compared with the available experimental data.

Mathematical modeling

The modeling for misfit and threading dislocations have been developed separately to analyze the different types of dislocations density (edge, screw and mixed) individually without graded layer as well as their effects on interlayers. A flow diagram shown in Fig. 1 presents a brief summary of mathematical modeling done for the proposed step-graded interlayer scheme. Details of this methodology will be discussed in the subsequent sections.

Critical thickness

The most basic form of InGaN heteroepitaxial growth consisting of a layer with constant indium (In) composition

is shown in Fig. 2a, which builds up strain with the increase of thickness. Such structure undergoes sudden relaxation with a large network of dislocations forming at the epilayer growth interface [16]. On the other hand, a step-graded interlayer technique is one, where the In composition in InGa_{1-x}N increases step wise up to the epilayer as shown in Fig. 2b. During the growth of each InGa_{1-x}N heteroepitaxy, the lattice as well as thermal expansion coefficient difference with substrate or previous interlayer introduces stain. This strain increases with thickness and after reaching a thickness, namely critical thickness (h_c), builds up enough strain energy to become energetically favorable to relax film through the formation of crystal defects, namely misfit dislocations. For any step-graded structure, multiple values of h_c are calculated for each interlayer and upper epilayer grown stepwise on GaN substrate as shown in Fig. 2b. These values of h_c can be

calculated for each layer using the Matthews-Blakeslee's well-known force balance model [16, 36]:

$$h_{ci} = \frac{b_i(1 - \nu_i \cos^2 \theta_i)}{8\pi(1 + \nu_i)|\varepsilon_{mi}| \sin \theta_i \sin \phi_i} \ln \left(\frac{h_{ci}}{r_{0i}} \right), \quad (1)$$

$$\varepsilon_{mi} = \frac{a_{i-1} - a_i}{a_{i-1}} \quad (2)$$

where the index i in subscript indicates number of interlayer, b is the length of burger vector, ν is the Poisson ratio, ϕ is the angle between the slip plane and normal to the film-substrate interface, θ is the angle between the dislocation line and burger vector, and r_0 is dislocation cut-off parameter. These parameters and the other basic parameters for the In_xGa_{1-x}N/GaN heteroepitaxy are listed in Table 1. The in-plane misfit strain between two successive layers will be calculated from Eq. (2). Multiple values of critical thickness will be found according to the parameters for each layer of the step-graded structures.

Slip systems in InGa_{1-x}N

In wurtzite InGa_{1-x}N, all the slip systems are not active for generation of misfit dislocation like cubic materials such as InGaAs or SiGe [41, 42]. Because all the planes do not experience a shear stress component due the lattice mismatch and should remain inactive in this configuration. Srinivasan et al. [43] estimated theoretically the appropriate slip systems for the MDs in wurtzite InGa_{1-x}N crystal as

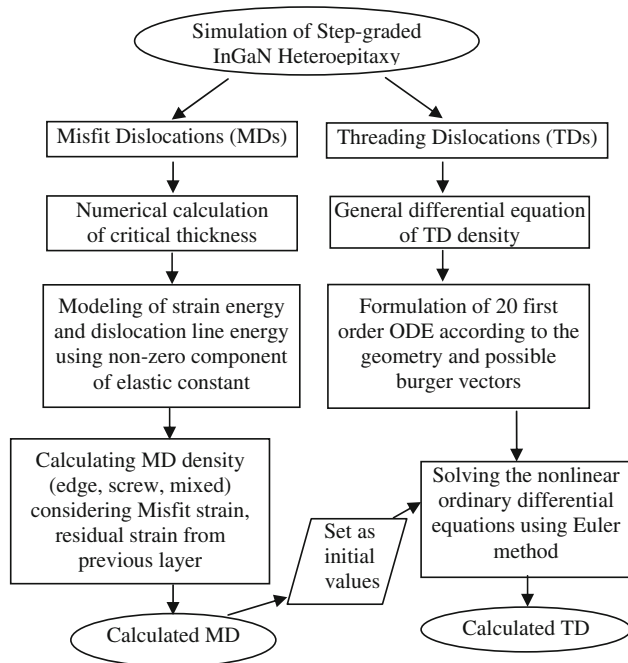


Fig. 1 A flow diagram for mathematical modeling of dislocations in step-graded InGa_{1-x}N heteroepitaxy

Fig. 2 Growth technique of wurtzite InGa_{1-x}N heteroepitaxy with **a** constant composition layer and **b** step-graded layer

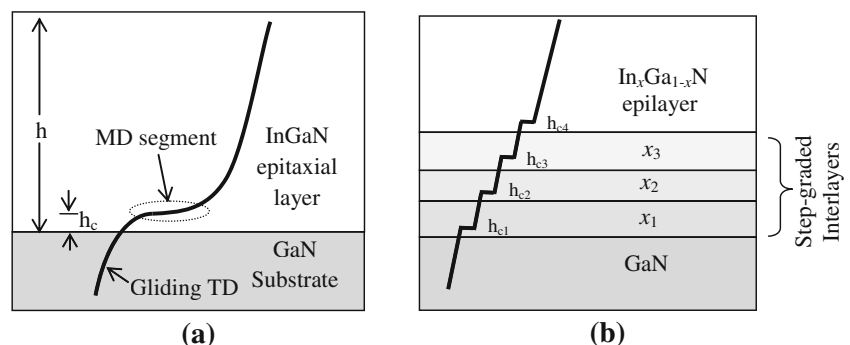


Table 1 Typical parameters for In_xGa_{1-x}N/GaN heteroepitaxy

Parameters	Values	Parameters	Values
a_{GaN}	3.1892 Å [55]	ϕ	Table 2
a_{InN}	3.5378 Å [56]	$\theta(\text{edge})$	90°
c_{GaN}	5.1850 Å [55]	$\theta(\text{screw})$	0°
c_{InN}	5.7033 Å [56]	$\theta(\text{mixed})$	60°
ν_{InN}	0.42 [47]	r_0	$b/2$ [47]
ν_{GaN}	0.35 [47]	r_A	500 Å [51]
b	Table 2	K_{xy}	[48]

Fig. 3 Slip systems for dislocation in InGaN lattice. **a** $1/3 \langle 11\bar{2}3 \rangle (11\bar{2}2)$, **b** $1/3 \langle 11\bar{2}3 \rangle (1\bar{1}01)$, and **c** $1/3 \langle 11\bar{2}0 \rangle (0001)$. Slip planes and directions are as indicated

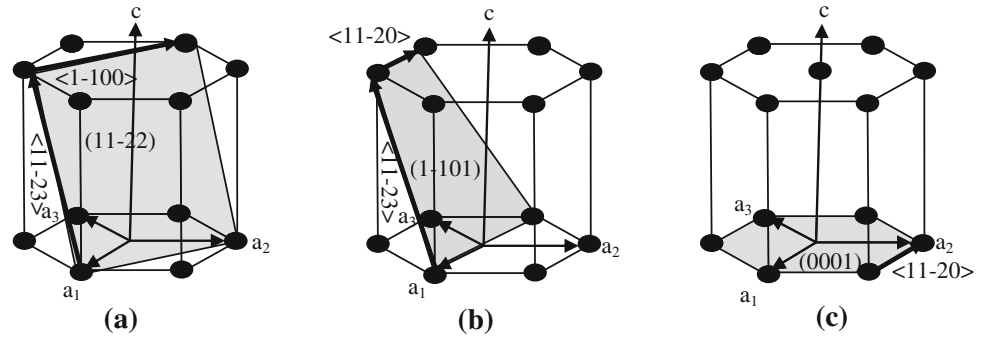


Table 2 Parameters of favored slip systems in wurtzite InGaN crystal structure showing b and ϕ

Possible slip	b	ϕ
$1/3 \langle 11\bar{2}3 \rangle (11\bar{2}2)$	$\sqrt{a^2(x) + c^2(x)}$	$\arctan \frac{a(x)}{c(x)}$
$1/3 \langle 11\bar{2}3 \rangle (1\bar{1}01)$	$\sqrt{a^2(x) + c^2(x)}$	$\arctan \frac{\sqrt{3}a(x)}{2c(x)}$
$1/3 \langle 11\bar{2}0 \rangle (0001)$	$\sqrt{3}a(x)$	90°

$1/3 \langle 11\bar{2}3 \rangle (11\bar{2}2)$ and $1/3 \langle 11\bar{2}3 \rangle (1\bar{1}01)$. However, there are also reports of pure a -type MDs which are theoretically the most efficient MD types for relieving the misfit strain [44]. Therefore, the basal plane slip system $1/3 \langle 11\bar{2}0 \rangle (0001)$ is also included for theoretical consideration. These three slip systems for wurtzite InGaN are shown in Fig. 3a, b, and c. The Table 2 listed the geometrical properties of these favored slip systems.

Misfit dislocations in step-graded InGaN

Initially the strain energy of the epitaxial film increases with thickness, and beyond the critical thickness some of this energy will be accommodated by the formation of misfit dislocation. In our previous works, we have developed an energy balance model for the step-graded structure to calculate the misfit dislocation density [45, 46]. It has been reported that the misfit strain in the heteroepitaxy starts to relax after h_c at each interlayer; the layer will be partially relaxed by MDs. In order to do this, the strain energy of each interlayer and energy accommodated by misfit dislocations have been calculated. One important term in that calculation was the consideration of residual strain using the nonzero component of elastic constant, after a thickness of h is [46, 47]

$$|\varepsilon_i| = \left| \varepsilon_{mi} - \left[\frac{3}{2} b_{ci} \rho_{MDi} \right] \right| \quad (3)$$

Therefore, the strain energy per unit area of the interface is

$$\frac{dW_i}{dA} = \left(c_{11} + c_{12} - \frac{2c_{13}^2}{c_{33}} \right) \left(|\varepsilon_{mi}| - \left[\frac{3}{2} b_{ci} \rho_{MDi} \right] \right)^2 h_i, \quad (4)$$

where c_{ij} are elastic constant of the film. The energy per unit length of a dislocation lying in the layer-substrate or layer-layer interface of a material with hexagonal symmetry can be written as [7, 8]

$$\frac{dE_{d(i)}}{d\ell} = b_{ci} \left(c_{11} + c_{12} - \frac{2c_{13}^2}{c_{33}} \right) \varepsilon_{mi} h_{ci} \left[\ln \left(\frac{h_i}{r_{0i}} \right) / \ln \left(\frac{h_{ci}}{r_{0i}} \right) \right] \quad (5)$$

The energy per unit interface area of an array of evenly distributed dislocations with spacing, l , is then $(1/l) (dE_{d(i)}/d\ell)$. As all three arrays of non-interacting MDs are assumed to be independent, the total energy per unit area may be expressed as

$$\begin{aligned} \frac{dE_i}{dA} &= \frac{3}{\ell} \frac{dE_{d(i)}}{d\ell} \\ &= \frac{3}{\ell} b_{ci} \left(c_{11} + c_{12} - \frac{2c_{13}^2}{c_{33}} \right) \varepsilon_{mi} h_{ci} \left[\ln \left(\frac{h_i}{r_{0i}} \right) / \ln \left(\frac{h_{ci}}{r_{0i}} \right) \right] h_i \end{aligned} \quad (6)$$

It is assumed that the dislocation spacing l is such that it minimizes the total energy within the i th interlayer. So the misfit dislocation density is found from $d(E_i + W_i)/dl = 0$ as

$$\begin{aligned} \rho_{MDi} &= \frac{1}{\ell_i^2} \\ &= \left\{ \begin{aligned} &\frac{2|\varepsilon_{mi}|}{3b_i \sin \theta \cos \phi} \left(1 - \frac{h_{ci} \ln(h_i/r_{0i})}{h_i \ln(h_{ci}/r_{0i})} \right) \quad \text{for } h_i \geq h_{ci} \\ &\left(\frac{2|\varepsilon_{mi}|}{3b_i \sin \theta \cos \phi} \right) \quad \text{for } h_i \leq h_{ci} \end{aligned} \right\} \end{aligned} \quad (7)$$

The layer grown upon the partially relaxed layer of thickness h_i will experience a misfit strain, $\varepsilon_{m(i+1)}$ reduced by the residual strain ε_i of the previous layer, where the value of ε_i is obtained from Eq. (3) for each interlayer. Therefore, MD density for each interlayer and epilayer will be updated with misfit strain as

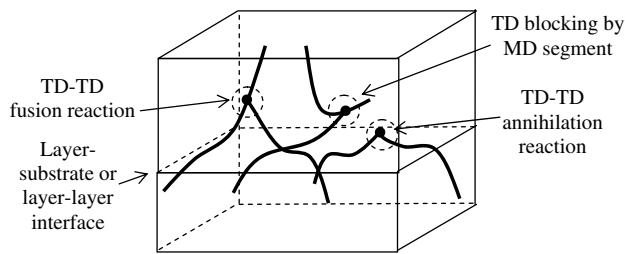


Fig. 4 Threading dislocation reduction mechanism in step-graded heteroepitaxy

$$|\varepsilon_{m(i+1)}| = \left| \frac{a_{l(i)} - a_{l(i+1)}}{a_{l(i)}} \right| - |\varepsilon_i| \quad (8)$$

Threading dislocations in step-graded InGaN

In the growth of lattice-mismatched heteroepitaxy, TDs are concomitantly generated with MDs. These TDs are non-equilibrium defects that always raise the internal energy of the film/substrate system [48]. Thus, there is a natural driving force to reduce the internal energy and TD density, subsequently. This reduction may occur due to annihilation and fusion reactions between pairs of inclined TDs and blocking by interaction between gliding TD with a MD line on its gliding plane [49]. All of these reactions have been shown schematically in Fig. 4. Annihilation reaction happens when two TD lines with equal and opposite burger vectors ($b_1 = -b_2$) undertake the reaction $b_1 + b_2 = 0$, removing the dislocations entirely. A fusion reaction occurs when two TD (b_1 and b_2) lines becomes one TD with new burger vector, $b_3 = b_1 + b_2$. However, both of these reactions can take place when the distance between interacting dislocations becomes smaller than the characteristic cross-section of a specific reaction: annihilation radius r_A for annihilation reaction and fusion radius r_F for fusion reactions [49, 50]. The general governing equation for TD density reduction of specific type ρ_x can be written for i th interlayer as

$$\left(\frac{d\rho_x}{dh} \right)_{i\text{th layer}} = \left(- \sum_y K_{xy} \rho_x \rho_y + \sum_l \sum_n K_{ln} \rho_l \rho_n - \sum_m \rho_x \rho_m \right)_{i\text{th layer}} \quad (9)$$

The first summation is for the annihilation and fusion reactions which reduce the TD density of x th type one per reaction. The second summation is for fusion reactions between the other type's l and n that produce the dislocation in the x th type, and the last one is for TD of x th type reduction

by MD blocking on its gliding path. The reaction kinetic coefficient K_{xy} presents the degree of possibility to participate in reaction of TDs type x and y in a particular interlayer that depends on the average differential motion between TDs with increasing film thickness. The values of the coefficients for a single layer are obtained using the general expression developed by Romanov et al. [48] as $K_{xy} = 2r_A [\sin \psi_x m_x - \sin \psi_y m_y]$, where ψ denotes the angle between TD line and surface normal and m indicates the direction of dislocation motion. Using this expression, the coefficient for each interlayer can be calculated for the different values of ψ and m corresponding to their mismatch strain. Though the mismatches strain in without graded layer is higher, the lateral motion of TDs with respect to interlayer thickness is larger for step-graded layer having comparatively lower stepped increase of thickness. Therefore, a multiple inclination of TDs at each interface enables them to increase the probability of interaction in step-graded structure.

In the InGaN heteroepitaxy, there are 20 unique families of dislocations according to their burger vectors and line directions [51]. Among them, numbers 1 to 6 are for edge dislocation whose burger vectors ($+a_1, -a_1, +a_2, -a_2, +a_3$ and $-a_3$) lie on the basal plane, numbers 7–18 are for mixed character ($+a_1+c, +a_1-c, -a_1+c, -a_1-c, +a_2+c, +a_2-c, -a_2+c, -a_2-c, +a_3+c, +a_3-c, -a_3+c$, and $-a_3-c$), and numbers 19–20 are for screw dislocation whose burger vectors ($+c$ and $-c$) are directed along c axis.

All possible annihilation and fusion reactions between TD–TD and TD–MD have been identified to write a reaction equation for a particular TD. For a specific case, TDs from family 1 can only have annihilation and fusion reactions with TDs from family 9, 10, 11, 12, 15, and 16 that reduce the TDs for the i th interlayer. So we can write

$$\left(\frac{d\rho_1}{dh} \right)_{i\text{th layer}} = (-K_{1,9}\rho_1\rho_9 - K_{1,10}\rho_1\rho_{10} - K_{1,11}\rho_1\rho_{11} - K_{1,12}\rho_1\rho_{12} - K_{1,15}\rho_1\rho_{15} - K_{1,16}\rho_1\rho_{16})_{i\text{th layer}} \quad (10)$$

In addition, TDs from family '1' may be generated within the i th interlayer only as the product of fusion reactions between TDs from the following pairs of families 7–8, 7–14, 7–18, 7–20, 8–13, 8–17, 8–19, 13–18, and 14–17. Therefore, for production of TDs from family 1 as a result of fusion, we can write

$$\left(\frac{d\rho_1}{dh} \right)_{i\text{th layer}} = \left(+2K_{7,8}\rho_7\rho_8 + K_{7,14}\rho_7\rho_{14} + K_{7,18}\rho_7\rho_{18} + K_{7,20}\rho_7\rho_{20} + K_{8,13}\rho_8\rho_{13} + K_{8,17}\rho_8\rho_{17} + K_{8,19}\rho_8\rho_{19} + K_{13,18}\rho_{13}\rho_{18} + K_{14,17}\rho_{14}\rho_{17} \right)_{i\text{th layer}} \quad (11)$$

Finally, the threading dislocation of family '1' could be blocked by edge type MD in the interlayer [49]. Therefore, TD reduction for type 1 due to this effect can be written as

$$\left(\frac{d\rho_1}{dh}\right)_{ith\ layer} = (-\rho_1\rho_m)_{ith\ layer} \quad (12)$$

Combining, the decrease of TD of type 1 as a result of annihilation (Eq. 10), increases due to fusion reaction (Eq. 11) and blocking by MDs (Eq. 12), we can arrive at the governing equation for the density of TD family '1' in the i th interlayer of step-graded InGa_{*N*} as

$$\left(\frac{d\rho_1}{dh}\right)_{ith\ layer} = \left(\begin{array}{l} \rho_1(k_{1,9}\rho_9 + K_{1,10}\rho_{10} + K_{1,11}\rho_{11} + K_{1,12}\rho_{12} + K_{1,16}\rho_{16}) \\ + 2K_{7,8}\rho_7\rho_8 + K_{7,14}\rho_7\rho_{14} + K_{7,18}\rho_7\rho_{18} + K_{7,20}\rho_7\rho_{20} + K_{8,13}\rho_8\rho_{13} \\ + K_{8,17}\rho_8\rho_{17} + K_{8,19}\rho_8\rho_{19} + K_{13,18}\rho_{13}\rho_{18} + K_{14,17}\rho_{14}\rho_{17} - \rho_1\rho_m \end{array} \right)_{ith\ layer} \quad (13)$$

Similarly, reaction equations for six different edge TDs, twelve mixed and two screw character TDs, i. e. a total of 20 first-order differential equations have been developed with corresponding burger vector and possible reaction for each interlayer of step-graded InGa_{*N*} heteroepitaxy.

Simulation results and discussion

Multilayer critical thickness

The simulation of the developed mathematical model and further optimization has been done using available numerical technique. The calculations have been done for a 1.5- μ m InGa_{*N*} step-graded layer using three interlayer each of 0.2 μ m with 10 % In composition difference and a final 0.9 μ m epilayer with In composition, $x = 0.4$. Multiple critical thicknesses for each interlayer and the upper epilayer have been calculated in different possible slip system for the step-graded InGa_{*N*} heteroepitaxy. Due to inverse relationship a slow increase in In composition in step-graded structure leads to larger h_c at each interface. Furthermore, the relative lattice mismatch between the adjacent interlayer has been considered according to Eq. (2), which makes the provision of larger values of h_c than that of the without graded layer. The critical thickness at different slip system with increasing In composition is plotted in Fig. 5. From the figure, the critical thicknesses have been found to be 12.4, 13.9, and 3.3 nm in (11-22), (1-101), and (0001) slip, respectively, for 10 % increase of In composition.

Misfit dislocations generation in InGa_{*N*}

At critical thicknesses the appearance of MDs are, for the first time, energetically favorable and start to relax the misfit strain. However, there is no reason to assume that all MDs will appear suddenly when the film thickness reaches h_c . Instead, after the critical thickness, MD density increases with increasing film thickness h [3]. Different types of MDs are calculated in step-graded In_{0.4}Ga_{0.6}N/GaN heteroepitaxy using three interlayers. Figure 6 shows the total MD generation in different slips as a function of layer thickness. All of the slips generate edge, screw, and

mixed dislocation depending on the angle between the burger vector and dislocation line direction. Figure 6a presents these three types of MDs separately in the $1/3 \langle 11-23 \rangle$ ($11-22$) slip of the step-graded In_{0.4}Ga_{0.6}N. The results in the $1/3 \langle 11-23 \rangle$ ($1-101$) and $1/3 \langle 11-20 \rangle$ (0001) slip systems are also shown in Fig. 6b, and c. The mixed MDs are considered as 60° types. There is a significant difference observed among the results where most of the MDs are of mixed types. It can be seen from the Fig. 6a that the total edge, screw, and mixed type MDs are of 4.74×10^{10} , 4.53×10^9 , and $4.03 \times 10^{11} \text{ cm}^{-2}$, respectively, generated on the first plane. From the above it is also observed that the MDs of any type generated in $1/3 \langle 11-20 \rangle$ (0001) slip are much

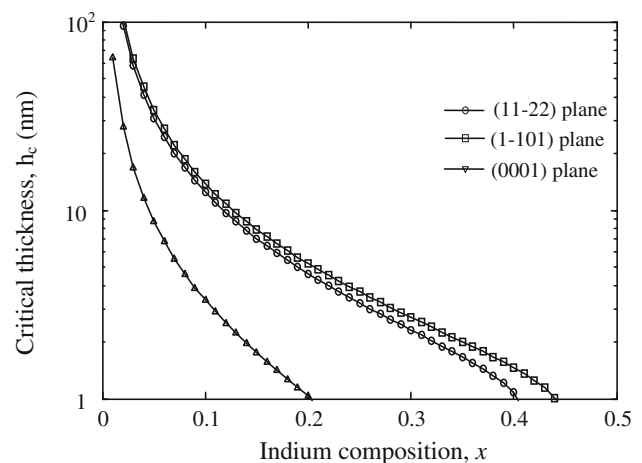


Fig. 5 The critical thickness in different slip systems of In_{*x*}Ga_{1-*x*}N/GaN heteroepitaxy

Fig. 6 The generation of different types of MDs on $1/3 < 11\bar{2}3 > (11\bar{2}2)$ slip of a step-graded InGaN ($\text{In}_{0.4}\text{Ga}_{0.6}\text{N}/\text{In}_{0.3}\text{Ga}_{0.7}\text{N}/\text{In}_{0.2}\text{Ga}_{0.8}\text{N}/\text{In}_{0.1}\text{Ga}_{0.9}\text{N}/\text{GaN}$) heteroepitaxy in different slip systems- **a** $1/3 < 11\bar{2}3 > (11\bar{2}2)$ slip, **b** $1/3 < 11\bar{2}3 > (1\bar{1}01)$ slip, and **c** $1/3 < 11\bar{2}0 > (0001)$ slip

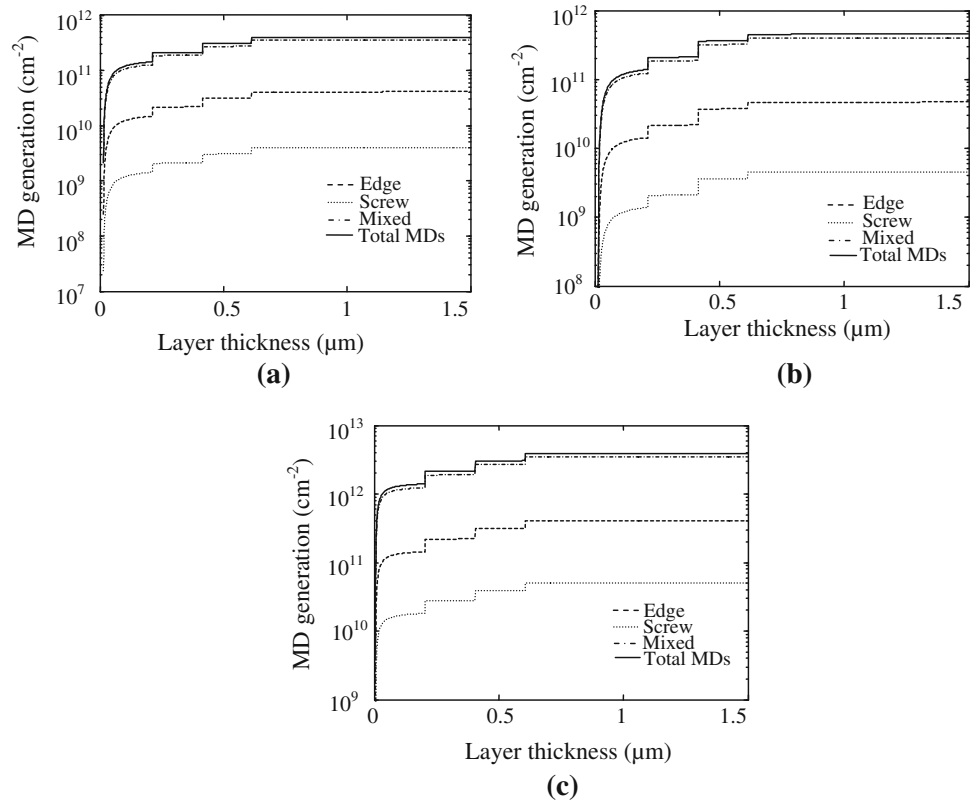
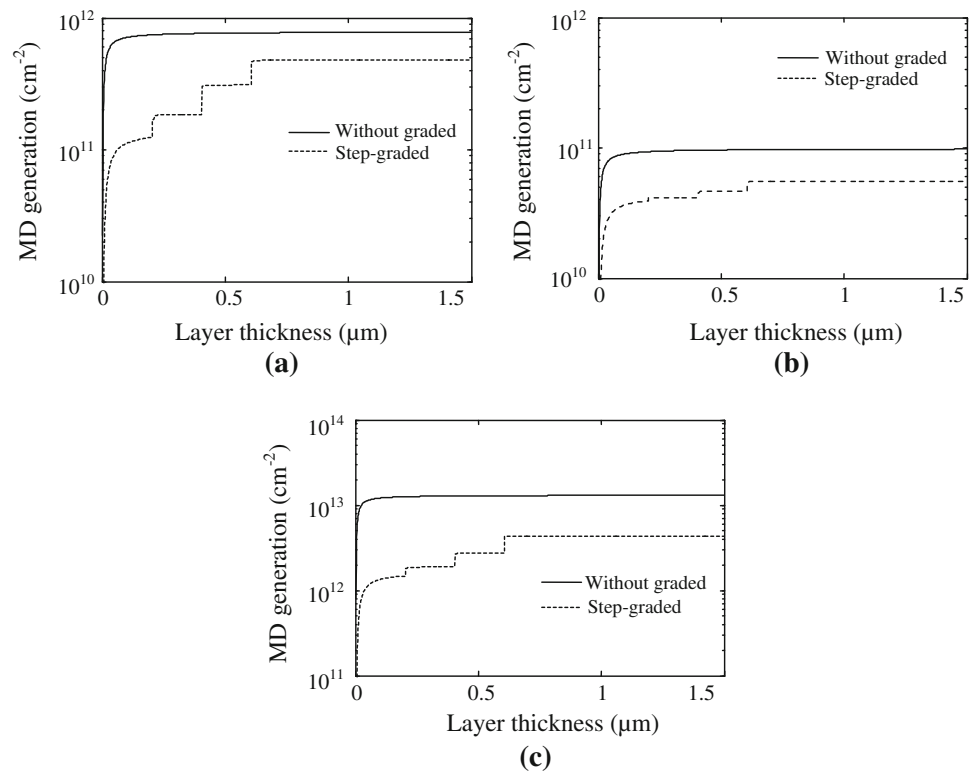


Fig. 7 Total MD generation of **a** edge **b** screw, and **c** mixed type in $\text{In}_{0.4}\text{Ga}_{0.6}\text{N}$ (step-graded)/GaN and $\text{In}_{0.4}\text{Ga}_{0.6}\text{N}$ (without graded)/GaN heteroepitaxy using three interlayers



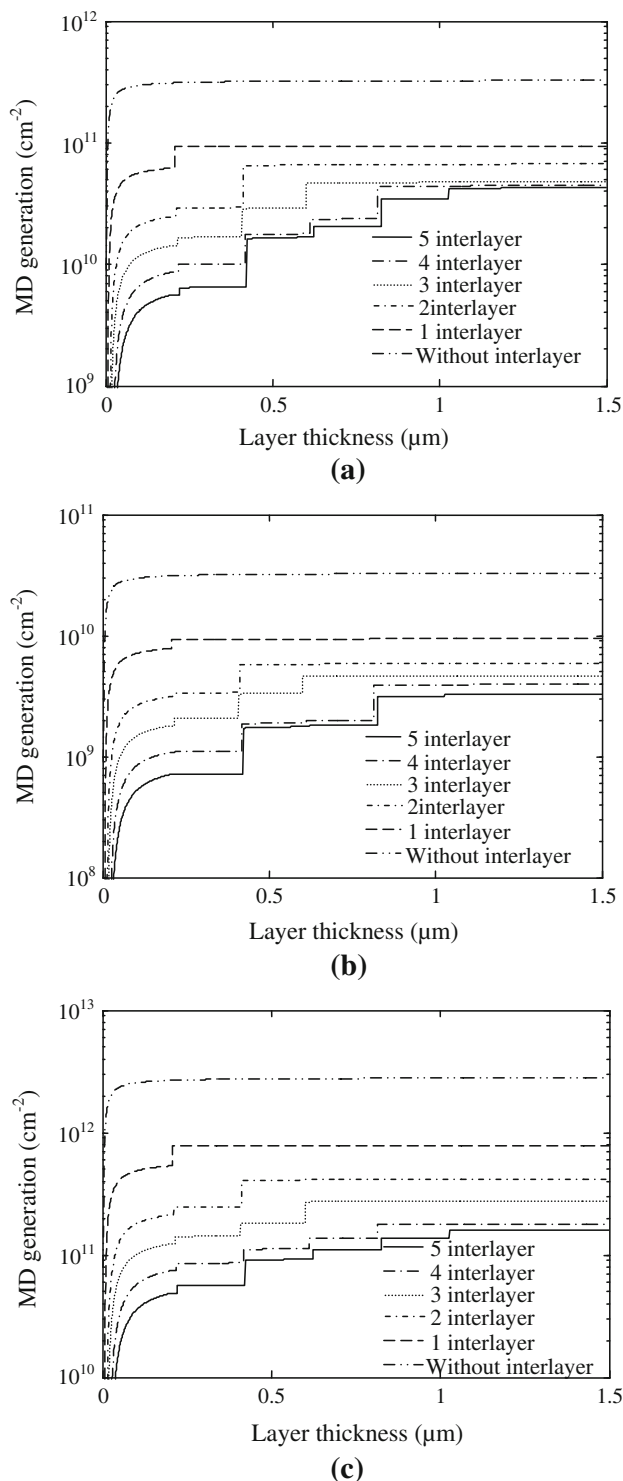


Fig. 8 Effects of interlayer number on **a** edge, **b** screw, and **c** mixed type of dislocations generation in $1/3 \langle 11\bar{2}3 \rangle$ ($11\bar{2}2$) slip of step-graded $\text{In}_{0.4}\text{Ga}_{0.6}\text{N}/\text{GaN}$ heteroepitaxy

higher than that of the other prismatic slips. This is because the hexagonal c-plane is isotropic and, therefore, burger vectors for all dislocation lines with different values of φ are equivalent. It is also clear from the above figures that

the mixed and edge type MDs have higher densities than the screw type ones. This is due to the comparatively lower energy requirement for mixed and edge type MDs than for the screw type ones.

Figure 7 presents the comparison of total generated edge, screw, and mixed type MDs in all possible planes of the step-graded and without graded structure. It is found from Fig. 7a that the total edge type MDs is 4.8×10^{11} and $7.8 \times 10^{11} \text{ cm}^{-2}$ for step-graded and without graded structure, respectively, considering $1.5 \mu\text{m}$ InGa_{0.4}N epilayer thickness. The significant difference of dislocation generation indicates that the step-graded interlayers successfully decrease the dislocation between GaN and InGa_{0.4}N interface. Though the reduction of screw type MDs as indicated in Fig. 7b due to step-graded interlayer is very small, a significant improvement has been observed in case of mixed type MDs as shown in Fig. 7c. The gradual application of misfit strain is primarily responsible for this improvement in dislocation density. With no interlayer the difference in mismatch between epilayer and substrate causes a large misfit and thermal strain between them. The large compressive stress also yields in the InGa_{0.4}N because of large thermal expansion coefficient for GaN ($5.5 \times 10^{-6} \text{ K}^{-1}$) than for InN ($4.0 \times 10^{-6} \text{ K}^{-1}$), resulting in an introduction of misfit lattice dislocations in the epilayer. On the other hand, with increasing the InGa_{0.4}N interlayer in a step-graded structure composition increases slowly step-wise. Thus the lattice as well as thermal expansion coefficient mismatch of the step-graded interlayer would be gradually change from GaN to $\text{In}_{0.4}\text{Ga}_{0.6}\text{N}$. Furthermore the misfit strain at the new interlayer could be compensated by the residual strain of opposite polarity from the previous layer. Therefore, the stress may be decreased or accommodated within a graded interlayer resulting in lower misfit dislocation.

In order to optimize the interlayer number for a specific structure, we have calculated MD densities at different interlayer numbers. Figure 8a, b and c shows the effect of increasing number of interlayer on edge, screw, and mixed type MDs, respectively, in $1/3 \langle 11\bar{2}3 \rangle$ ($11\bar{2}2$) slip system of the $\text{In}_{0.4}\text{Ga}_{0.6}\text{N}/\text{GaN}$ heteroepitaxy. We have estimated the densities from 0 to 5 interlayers with the same final In composition ($x = 0.4$). The edge MD densities of 3.25×10^{11} , 9.39×10^{10} , 6.7×10^{10} , 4.74×10^{10} , 4.45×10^{10} and $4.24 \times 10^{10} \text{ cm}^{-2}$ have been calculated for without, 1, 2, 3, 4 and 5 interlayer, respectively. Similar improvements have been evaluated for other types of MDs in all slips. From the results it can be seen that a significant improvement of epilayer quality can be achieved with increasing number of interlayer up to 4 where 8 % indium composition differences have been used for each interlayer. The epilayer is further improved for five inter layers but the improvement tendency is very low. In addition, increasing more and more interlayers can

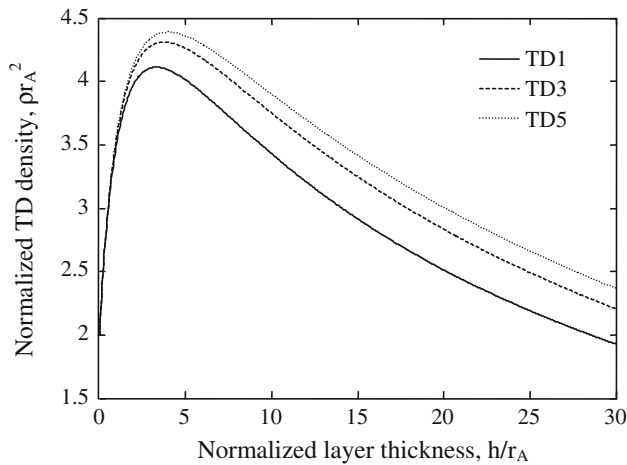


Fig. 9 The variation of edge type TD density with specific number in step-graded $\text{In}_{0.4}\text{Ga}_{0.6}\text{N}/\text{GaN}$ system

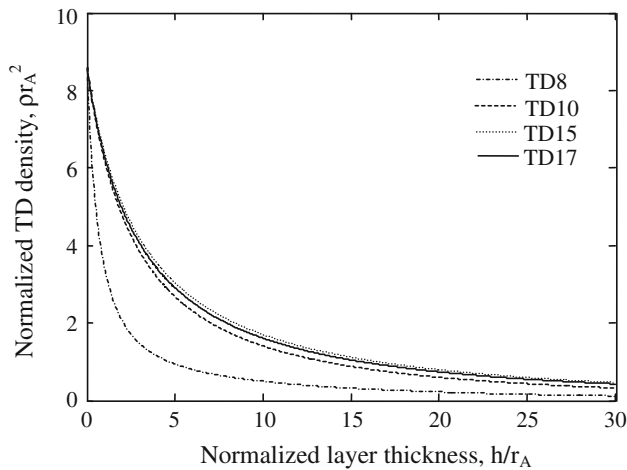


Fig. 10 The variation of mixed type TD density with specific number in step-graded $\text{In}_{0.4}\text{Ga}_{0.6}\text{N}/\text{GaN}$ system

increase the experimental complexity and will introduce interfacial dislocations each layer. These results are consistent with the outcomes of improved InGaN epilayer quality using step-graded interlayer according to Islam et al. [23], who have shown that inserting more inter layer with 3–5 % indium composition difference did not decrease the dislocations further. Therefore, it is reasonable to conclude that the insertion of interlayer is found effective where the In composition difference between the under layer and epi-layer is around 6.5–8 %.

Threading dislocations in wurtzite InGaN

The threading dislocation densities in the step-graded InGaN heteroepitaxy have been evaluated from the numerical simulation of the reaction model. A total of 20 first orders, nonlinear differential equations according to all possible

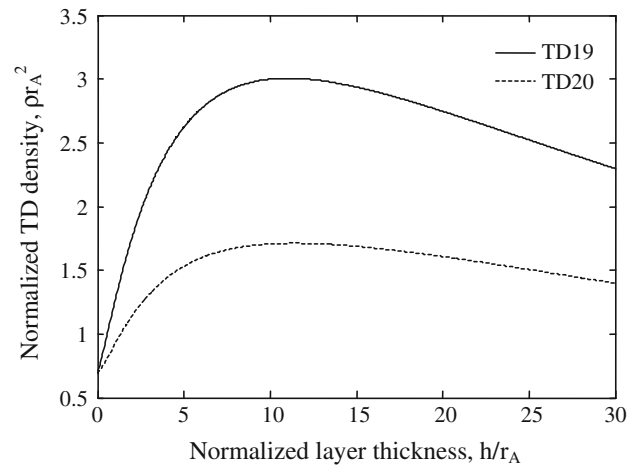


Fig. 11 The variation of screw type TD density with specific number in step-graded $\text{In}_{0.4}\text{Ga}_{0.6}\text{N}/\text{GaN}$ system

burger vectors have been solved for the same structure of $\text{In}_{0.4}\text{Ga}_{0.6}\text{N}$. To execute the solution, the MDs are considered as the main source of TDs of specific types to set the initial values. The reaction kinetic coefficients between each pair of TDs have been determined for each interlayer considering the annihilation and fusion reaction radius of 500 Å. The solution presents the variation of TD densities with increasing film thickness. Figure 9 shows the density reduction of TD 1, 3, and 5 (edge type) in the step-graded $\text{In}_{0.4}\text{Ga}_{0.6}\text{N}$. It can be reported from the figure that initially the edge type TDs increase rapidly and then begin to decrease with increasing film thickness. The initial increase is due to their lower initial values and their generation from the reaction of other types is higher. Figures 10 and 11 present the variation of mixed and screw type TD densities, respectively, with specific number as a function of film thickness for the step-graded structure. The mixed type TD decreases monotonically with increasing film thickness and these decreases are quicker than any other type of TD. This is because, though the screw dislocations are considered very low initial values, they can be the product of other reaction and allowed to participate in reaction with other TDs. As a result, both the screw-mixed reaction producing vertical edge dislocation and the edge-mixed reaction producing vertical screw dislocations. Therefore, the mixed TD density becomes so low as to prevent the further interaction among TDs, with the end result of saturation in TD density. The nature of screw type TDs are different from that of others. Though both TDs increase with thickness, TD 19 has higher rate than TD 20. The improvement in TD density in the top surface of the epi-layer has been understood from the comparison of Fig. 12a, and b. These figures show the decrease of average edge, mixed, and screw TD densities of the step-graded and without graded $\text{In}_{0.4}\text{Ga}_{0.6}\text{N}$ heteroepitaxy, respectively.

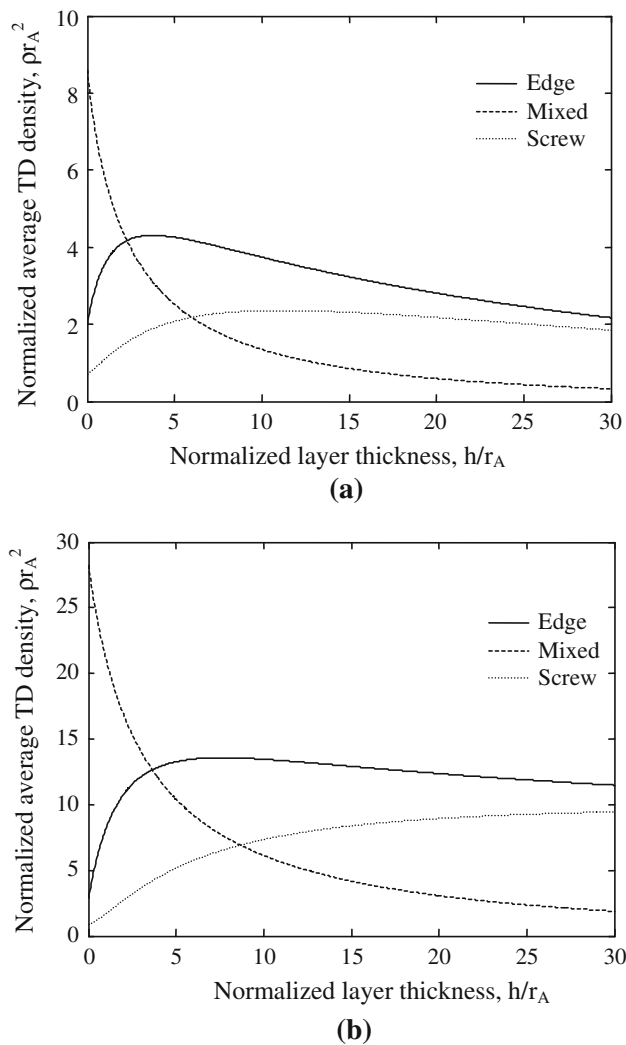


Fig. 12 The average edge, screw and mixed type TDs for- **a** $\text{In}_{0.4}\text{Ga}_{0.6}\text{N}(\text{step-graded})/\text{GaN}$ and **b** $\text{In}_{0.4}\text{Ga}_{0.6}\text{N}(\text{without graded})/\text{GaN}$ system

The total edge, screw, and mixed type TD densities for the step-graded structures are found to be 8.88×10^{10} , 7.4×10^{10} , and $1.32 \times 10^{10} \text{ cm}^{-2}$, respectively, at the top surface of the epilayer, whereas these values are 4.6×10^{11} , 3.78×10^{11} , and $7.52 \times 10^{10} \text{ cm}^{-2}$, respectively, for the without graded structure.

There are several reasons behind these improvements in epilayer quality of the step-grade structure. Since the dislocations from the substrate are extremely much lower than the dislocation generated from other sources, the MDs are considered as the main source of TDs. In case of without graded structure the most of the MDs are generated near the film–substrate interface due to large mismatch and lower critical thickness. Therefore, the TDs that glided in the upper layers could not be blocked by the MDs. On the other hand, the MDs' generations in the step-graded structure spread throughout the entire layer instead of being

concentrated in a single interface. As a result, the TDs that glided out from the first interlayer could be blocked by MDs generated in the second interlayer or TDs from second layer may be blocked by MDs in upper layer and so on. Therefore, the TD reduction in step-graded structure can be enhanced by the MD blocking. Moreover, as the strain inside the thin film drives threading dislocations to incline at each interface and react with each other, the introduction of an intentionally strained layer can be used to facilitate the TDs reduction process. This is the basic of TD reduction mechanism in step-graded layer. Bending of dislocations in without graded structure only occurs very close to the $\text{In}_x\text{Ga}_{1-x}\text{N}/\text{GaN}$ interface, whereas dislocation bending can be noticed at each interface between InGaN interlayers of different composition in step-graded structure [52]. Moreover, due to large misfit dislocation density a strong interaction force among them prohibits the glide motion of the dislocation and further relaxation in without graded layer. Therefore, it requires further dislocation nucleation to relax the strain resulting higher TD densities in epilayer. On the other hand, lower MD densities offers weak interaction force with easy gliding of TDs. A well-designed graded layer should relax the misfit strain mostly through the glide motion of existing threading dislocations instead of nucleation of new dislocation. Furthermore, as observed in various experimental works most nucleation sites for TDs are MDs which are extremely lower in step-graded structure than the without graded.

Experimental evidence

Growth procedure

The films are grown on (0001) sapphire substrate using the metal organic vapor phase epitaxy (MOVPE) with a horizontal reactor. The $\text{In}_x\text{Ga}_{1-x}\text{N}$ heteroepitaxy is grown on GaN template using two interlayers having intermediate In compositions between epilayer and template. Triethylgallium (TEG), trimethylindium (TMI), and ammonia (NH_3) are used as Gallium (Ga), Indium (In), and Nitrogen (N) sources, respectively. The complete growth procedure of graded layer hetero-structure can be seen from the time chart shown in Fig. 13. At first GaN template of about $2 \mu\text{m}$ is grown at $1,000^\circ\text{C}$. Then step-graded $\text{In}_x\text{Ga}_{1-x}\text{N}$ films with different In compositions are grown as interlayers between the GaN template and InGaN epi-layer. The thickness of each interlayer is (150–200 nm) kept more than the critical thickness corresponding to the In composition. Finally, InGaN epi-layer with thickness $\sim 1.5 \mu\text{m}$ is grown at pressure 150 Torr. The growth temperatures are kept from 750 to 900°C depending on the optimal growth conditions required for various $\text{In}_x\text{Ga}_{1-x}\text{N}$ layers with

Fig. 13 Time chart for the epitaxial growth of InGaN with step-graded interlayer

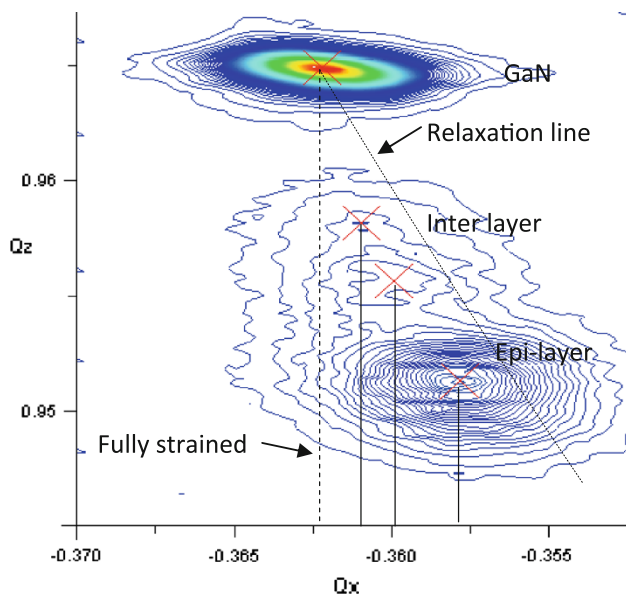
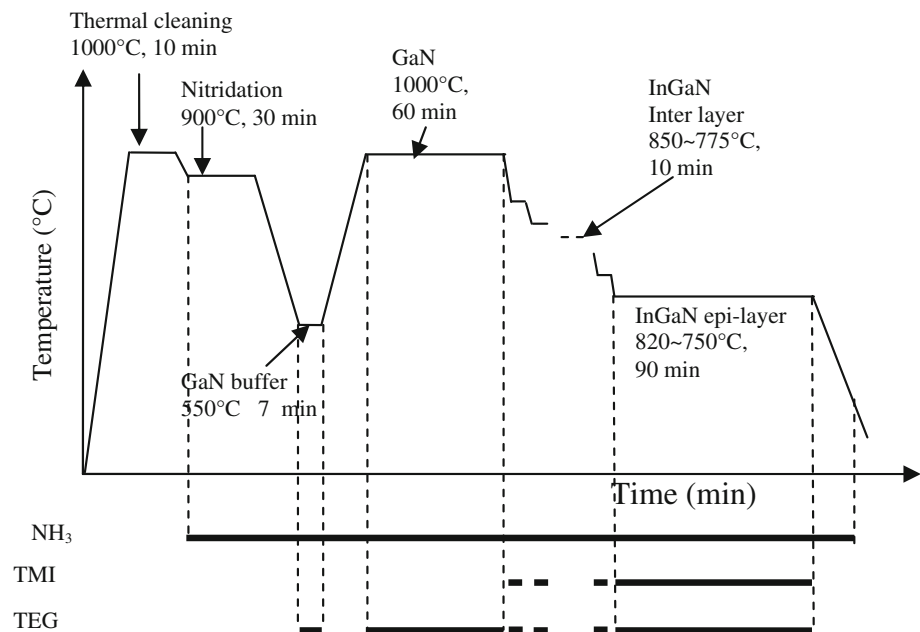


Fig. 14 Reciprocal space maps for the (10-15) reflections of InGaN epi-layer with two inter layers

different In compositions. The In compositions of inter-layer and epi-layer are controlled changing the growth temperature [53]. Growth interrupts are employed between the growths of two consecutive interlayers having different In compositions and allowing thermal annealing under NH_3 . Also during the growth interrupt, the substrate temperature is adjusted to the optimum value required for the growth of each $\text{In}_x\text{Ga}_{1-x}\text{N}$ layer. More details about experimental procedure have been discussed in [23].

Experimental observation of relaxation

Information on the crystal structure and strain of an epitaxial film can be obtained by performing a RSM on an asymmetric reflection using a double-crystal X-ray diffraction system. Additionally, the out-of-plane, c and in-plane, a lattice constant of the hexagonal structure can be measured and a direct comparison of the position of GaN template, InGaN inter layers, and epi-layer diffraction peaks in the RS can be performed. A RSM of the $\text{In}_{0.14}\text{Ga}_{0.86}\text{N}$ epi-layer with two inter layers $\text{In}_{0.05}\text{Ga}_{0.95}\text{N}$ and $\text{In}_{0.09}\text{Ga}_{0.91}\text{N}$, measured around the (10-15) reflection is shown in Fig. 14. The thickness of each inter layer and the epi-layer is around 0.15 and 1.5 μm , respectively. Fully strained and relaxed lines are also shown. The relaxation line has been drawn calculating the lattice constant of InGaN using the relation [54], where the input parameters necessary to complete the calculation are the GaN ($c_{\text{GaN}}0.51850$, $a_{\text{GaN}}0.31892$ nm) [55] and InN ($c_{\text{InN}}0.57033$, $a_{\text{InN}}0.35378$ nm) [56] relaxed lattice constants. The RSM confirms the two inter layers and the epi-layer peaks by the diffraction profile of the InGaN film. It can be seen from the Fig. 14 that the InGaN epi-layers are not completely relaxed, while the interlayers show comparatively more strain. The lattice mismatch of GaN template to 1st inter layer, 1st inter layer to 2nd inter layer, and 2nd inter layer to InGaN epi-layer is 0.33, 0.31, and 0.59 %, respectively, whereas the calculated lattice mismatch of completely relaxed InGaN sample with the same In composition is 1.35 % for without graded layer. Therefore, the step-graded interlayer with the step-by-step

relaxation of InGaN epi-layer decreases the lattice mismatch gradually that can reduce the defect density.

Comparison between simulated and experimental results

The result comparison with experimental work is an essential task for validation of any model. Experimental measurements of dislocations have been performed on the sample grown in laboratory. It has been reported that the dislocation density, particularly the edge dislocations, decreases considerably with the insertion of interlayers for higher In composition [23]. An edge dislocation of $3.37 \times 10^{10} \text{ cm}^{-2}$ is obtained for a sample with compositionally two step-graded interlayers ($\text{In}_{0.06}\text{Ga}_{0.94}\text{N}$ and $\text{In}_{0.13}\text{Ga}_{0.87}\text{N}$) and $1.5 \mu\text{m}$ $\text{In}_{0.26}\text{Ga}_{0.74}\text{N}$ final epilayer. On the other hand, using the developed model the edge dislocation density of $2.61 \times 10^{10} \text{ cm}^{-2}$ has been evaluated in (11–22) plane of a $1.5\text{-}\mu\text{m}$ step-graded $\text{In}_{0.26}\text{Ga}_{0.74}\text{N}$ heteroepitaxy using two interlayers. In contrast to lattice mismatch calculated from the RSM, we have also estimated the strain relaxation profile for a $1.5\text{-}\mu\text{m}$ $\text{In}_{0.14}\text{Ga}_{0.86}\text{N}$ epilayer using our model with two interlayers having same composition as Fig. 14. It has been found that the mismatches of 0.32, 0.33, and 0.58 % are estimated in first interlayer to GaN substrate, second interlayer to first interlayer, and epilayer to second interlayer, respectively.

Conclusions

From the above realization it can be summarized that a proper management of magnitude and rate of misfit strain is the key requirement to control the misfit and threading dislocations during the growth of InGaN. In this work, the step-graded interlayer technique for wurtzite InGaN heteroepitaxy has been investigated through mathematical modeling and numerical simulation as well as experimental observation for future solar cells.

The multilayer epitaxial structures with 40 % In composition for $\text{In}_x\text{Ga}_{1-x}\text{N}$ has been considered using step-graded structure. It has been demonstrated that the insertion of step-graded interlayers significantly reduces the mixed and edge MDs up to a certain number within a specific In composition. It has been found that no significant misfit dislocation density decreases for the heteroepitaxy with In composition difference below 8 %. These results are consistent with the reported results of improved InGaN epilayer quality using step-graded interlayer. In addition, a numerical solution of TDs' reaction models has confirmed their diminishing densities with increasing thickness. The less nucleation sites for TDs and step inclination at each interlayer of the step-graded structure result in significant

improvement in the epilayer quality with extremely less TD density, especially of mixed type. The edge and screw dislocations evaluated using this model in (11–22) plane have been found to agree well with the experimentally measured result for InGaN film using step-graded interlayer. The model verification has also been confirmed by comparing the lattice mismatch from the model and measured from RSM.

The above realizations indicate the potentiality of step-graded interlayer technique for InGaN heteroepitaxy. This simulation methodology can be used for other wurtzite heteroepitaxial material to estimate the performance of future high-efficiency solar cells.

Open Access This article is distributed under the terms of the Creative Commons Attribution License which permits any use, distribution, and reproduction in any medium, provided the original author(s) and the source are credited.

References

1. Kong, Y.C., Zheng, Y.D., Zhou, C.H., Deng, Y.Z., Shen, B., Gu, S.L., Zhang, R., Han, P., Jiang, R.L., Shi, Y.: A novel $\text{In}_x\text{Ga}_{1-x}\text{N}/\text{InN}$ heterostructure field effect transistor with extremely high two-dimensional electron-gas sheet. *Solid. State. Elec.* **49**(2), 199–203 (2005)
2. Nanishi, Y., Saito, Y., Yamaguchi, T.: RF-Molecular beam epitaxy growth and properties of InN and related alloys. *Jpn. J. Appl. Phys.* **42**(5A), 2549 (2003)
3. Wu, J., Walukiewicz, W., Yu, K.M., Shan, W., Ager III, J.W., Haller, E.E., Lu, H., Schaff, W.J., Metzger, W.K., Kurtz, S.: Superior radiation resistance of $\text{In}_{1-x}\text{Ga}_x\text{N}$ alloys: Full-solar-spectrum photovoltaic material system. *J. Appl. Phys.* **94**(10), 6477–6482 (2003)
4. Hasan, M.T., Kaysir, M.R., Islam, M.S., Bhuiyan, A.G., Islam, M.R., Hashimoto, A., Yamamoto, A.: 2DEG properties in InGaN/InN/InGaN-based double channel HEMTs. *Phys. Stat. Sol. C* **7**(7–8), 1997–2000 (2010)
5. Lin, C.F., Zheng, J.H., Yang, Z.J., Dai, J.J., Lin, D.Y., Chang, C.Y., Lai, Z.X., Hong, C.S.: High-efficiency InGaN-based light-emitting diodes with nonporous GaN: Mg structure. *Appl. Phys. Lett.* **88**(8), 083121–083123 (2006)
6. Yamamoto, A., Islam, M.R., Kang, T.T., Hashimoto, A.: Recent advances in InN-based solar cells: status and challenges in InGaN and InAlN solar cells. *Phys. Stat. Sol. C* **7**(5), 1309–1316 (2010)
7. Neufeld, C.J., Toledo, N.G., Cruz, S.C., Lza, M., DenBaars, S.P., Mishra, U.K.: High quantum efficiency InGaN/GaN solar cells with 2.95 eV band gap. *Appl. Phys. Lett.* **93**, 143502–143503 (2008)
8. Horng, R.H., Lin, S.T., Tsai, Y.L., Chu, M.T., Liao, W.Y., Wu, M.H., Lin, R.M., Lu, Y.C.: Improved conversion efficiency of GaN/InGaN thin-film solar cells. *IEEE Elec. Device Lett.* **30**(7), 724–726 (2009)
9. Liu, Y.: Heteroepitaxial growth of InN and InGaN alloys on GaN(0001) by molecular beam epitaxy. Postgraduate thesis, the University of Hong Kong, Hong Kong (2005)
10. Cho, H.K., Lee, J.Y., Kim, K.S., Yang, G.M.: Formation of misfit dislocations and stacking faults in high indium content $\text{In}_x\text{Ga}_{1-x}\text{N}$ layers grown by metal organic chemical vapor deposition. *J. Korean Phys. Soc.* **39**, S165–S169 (2001)



11. Wang, H., Jiang, D.S., Jahn, U., Zhu, J.J., Zhao, D.G., Liu, Z.S., Zhang, S.M., Qiu, Y.X., Yang, H.: Investigation on the strain relaxation of InGaN layer and its effects on the InGaN structural and optical properties. *Phys. B* **405**, 4668–4672 (2010)
12. Cho, H.K., Yang, G.M.: Generation of misfit dislocations in high indium content InGaN layer grown on GaN. *J. Crystal Growth* **243**(1), 124–128 (2002)
13. Song, M., Wu, Z., Fang, Y., Xiang, R., Sun, Y., Wang, H., Yu, C., Xiong, H., Dai, J., Chen, C.: Improved photovoltaic performance of InGaN single junction solar cells by using n-on-p type device structure. *J. Optoelectron. Adv. Mater.* **12**(7), 1452–1456 (2010)
14. Look, D.C., Sizelove, J.R.: Dislocation scattering in GaN. *Phys. Rev. Lett.* **82**, 1237–1240 (1999)
15. Sasaoka, C., Sunakawa, H., Kimura, A., Nido, M., Usui, A., Sakai, A.: High-quality InGaN MQW on low-dislocation-density GaN substrate grown by hydride vapor-phase epitaxy. *J. Crystal Growth* **189**(190), 61–66 (1998)
16. Matthews, J.W., Blakeslee, A.E.: Defects in epitaxial multilayer: 1. Misfit dislocation. *J. Crystal Growth* **27**, 118–125 (1974)
17. Ayers, J. E.: ©2007 by Taylor & Francis Group, LLC, pp. 180–189, ISBN 0-8493-7195-3 (2007)
18. Hanada, T., Shimada, T., Ji, S.Y., Hobo, K., Liu, Y., Matsuoka, T.: Strain relaxation mechanism of InGaN thin film grown on m-GaN. *Phys. Stat. Sol. C* **8**(2), 444–446 (2011)
19. Gmili, Y.E., Orsal, G., Pantzas, K., Ahaitouf, A., Moudakir, T., Gautier, S., Patriarche, G., Troadec, D., Salvestrini, J.P., Ougazaden, A.: Characteristics of the surface microstructures in thick InGaN layers on GaN. *Opt. Mat. Express* **3**(8), 1111–1118 (2013)
20. Kasper, E., Lyutovich, K.: Strain adjustment with thin virtual substrates. *Sol. State Elect.* **48**(8), 1257–1263 (2004)
21. Ee, Y.K., Biser, J.M., Cao, W., Chan, H.M., Vinci, R.P., Tansu, N.: Metalorganic vapor phase epitaxy of III-Nitride light-emitting diodes on nanopatterned AGOG sapphire substrate by abbreviated growth mode. *IEEE J. Sel. Top. Quantum Electr.* **15**, 1066–1072 (2009)
22. Ee, Y.K., Li, X.H., Biser, J., Cao, W., Chan, H.M., Vinci, R.P., Tansu, N.: Abbreviated MOVPE nucleation of III-nitride light-emitting diodes on nano-patterned sapphire. *J. Crys. Growth* **312**, 1311–1315 (2010)
23. Islam, M.R., Ohmura, Y., Hashimoto, A., Yamamoto, A., Kinoshita, K., Koji, Y.: Step-graded interlayers for the improvement of MOVPE In_xGa_{1-x}N ($x \sim 0.4$) epi-layer quality. *Phys. Stat. Sol. C* **7**(7–8), 2097–2100 (2010)
24. Nakamura, S., Jayavel, P., Koyama, T., Hayakawa, Y.: Investigations on the effect of InSb and InAsSb step-graded buffer layers in InAs_{0.5}Sb_{0.5} epilayers grown on GaAs (001). *J. Crystal Growth* **300**, 497–502 (2007)
25. Bertoli, B., Sidoti, D., Xhuxhi, S., Kujofsa, T., Cheruku, S., Correa, J.P., Rago, P.B., Suarez, E.N., Jain, F.C., Ayers, J.E.: Equilibrium strain and dislocation density in exponentially graded Si_{1-x}Ge_x/Si (001). *J. Appl. Phys.* **108**(11), 113525-5 (2010)
26. Ocampo, J.F., Suarez, E., Jain, F.C., Ayers, A.E.: Overshoot graded layers for mismatched heteroepitaxial devices. *J. Elect. Mat.* **37**, 1035 (2008)
27. Ayers, J.E.: Multiple critical layer thicknesses in retro-graded heterostructures. *Appl. Phys. Lett.* **92**, 102104-3 (2008)
28. Fitzgerald, E.A.: Dislocations in strained-layer epitaxy: theory, experiment, and applications. *Mats. Sci. Reports* **7**, 87 (1991)
29. Fitzgerald, E.A., Kim, A.Y., Currie, M.T., Langdo, T.A., Tarschi, G., Bulsara, M.T.: Dislocation dynamics in relaxed graded composition semiconductor. *Mat. Sci. Engg.* **B67**, 53–61 (1999)
30. Bertoli, B., Suarez, N., Ayers, J.E., Jain, F.C.: Misfit dislocation density and strain relaxation in graded semiconductors with arbitrary composition profiles. *J. Appl. Phys.* **106**, 073519-7 (2009)
31. Romanov, A.E., Pompe, W., Mathis, S., Beltz, G.E., Speck, J.S.: Threading dislocation reduction in strained layers. *J. Appl. Phys.* **85**, 182–192 (1999)
32. Manning, I.C., Weng, X., Acord, J.D., Fanton, M.A., Snyder, D.W., Redwing, J.M.: Tensile stress generation and dislocation reduction in Si-doped Al_xGa_{1-x}N films. *J. Appl. Phys.* **106**, 023506 (2009)
33. Manning, I.C., Weng, X., Fanton, M.A., Snyder, D.W., Redwing, J.M.: Effects of composition on dislocation microstructure and stress in Si-doped Al_xGa_{1-x}N. *J. Crys. Growth* **312**, 1301–1306 (2010)
34. Mooney, P.M., Jordan-Sweet, J.L., Chu, J.O., LeGoues, F.K.: Evolution of strain relaxation in step-graded SiGe/Si structures. *Appl. Phys. Lett.* **66**, 3642–3644 (1995)
35. Krishnamoorthy, V., Lin, Y.W., Park, R.M.: Application of 'critical compositional difference concept to growth of low dislocation density ($<10^4/\text{cm}^2$) In_xGa_{1-x}As ($x \leq 0.5$) on GaAs. *J. Appl. Phys.* **72**, 1752–1757 (1992)
36. Macpherson, G., Beanland, R., Goodhew, J.P.: A novel design method for the suppression of edge dislocation formation in step-graded InGaAs/GaAs layers. *Philos. Mag. A* **73**(05), 1439–1450 (1996)
37. Zhang, J., Tansu, N.: Improvement in spontaneous emission rates for InGaN quantum wells on ternary InGaN substrate for light-emitting diodes. *J. Appl. Phys.* **110**, 113110 (2011)
38. Zhang, J., Tansu, N.: Optical gain and laser characteristics of InGaN quantum wells on ternary InGaN substrates. *IEEE Photonics J.* **5**, 2600111 (2013)
39. Kotani, T., Lugli, P., Hamaguchi, C.: Optical gain analysis of c-InGaN quantum wells on unstrained c-In_{0.31}Ga_{0.69}N templates. *Appl. Phys. Lett.* **102**, 011128 (2013)
40. Zhao, H., Liu, G., Zhang, J., Poplawsky, J.D., Dierolf, V., Tansu, N.: Approaches for high internal quantum efficiency green InGaN light-emitting diodes with large overlap quantum wells. *Opt. Express* **19**(S4), A991–A1007 (2011)
41. Tyagi, A., Wu, F., Young, E.C., Chakraborty, A., Ohta, H., Bhat, R., Fujito, K., DenBaars, S.P., Nakamura, S., Speck, J.S.: Partial strain relaxation via misfit dislocation generation at heterointerfaces in (Al, In)GaN epitaxial layers grown on semipolar (11–22) GaN free standing substrates. *Appl. Phys. Lett.* **95**, 251905 (2009)
42. Young, E.C., Wu, F., Romanov, A.E., Tyagi, A., Gallinat, C.S., DenBaars, S.P., Nakamura, S., Speck, J.S.: Lattice tilt and misfit dislocations in (11–22) semi polar GaN Heteroepitaxy. *Appl. Phys. Exp.* **3**, 011004 (2010)
43. Srinivasan, S., Geng, L., Ponce, F.A., Narukawa, Y., Tanaka, S.: Slip systems and misfit dislocations in InGaN epilayers. *Appl. Phys. Lett.* **83**(25), 5187–5189 (2003)
44. Vennegues, P., Bougrioua, Z., Bethoux, J.M., Azize, M., Tottereau, O.: Relaxation mechanisms in metal-organic vapor phase epitaxy grown Al-rich (Al, Ga)N/GaN heterostructures. *J. Appl. Phys.* **97**(2), 024912–024916 (2005)
45. Hossain, M.A., Hasan, M.M., Islam, M.R.: Strain relaxation via misfit dislocation in step-graded InGaN heteroepitaxial layers grown on semipolar (11–22) and (1–101) GaN. *Int. J. Appl. Phys. Math.* **02**(01), 049–053 (2012)
46. Hossain, M.A., Islam, M.R.: A theoretical calculation of misfit dislocation and strain relaxation in step-graded In_xGa_{1-x}N/GaN layers. *Adv. Mat. Res.* **403–408**, 456 (2012)
47. Holec, D., Costa, P.M.F.J., Kappers, M.J., Humphreys, C.J.: Critical thickness calculations for InGaN/GaN. *J. Crystal Growth* **303**, 314–317 (2007)
48. Romanov, A.E., Pompe, W., Beltz, G., Speck, J.S.: Modeling of threading dislocation density reduction in heteroepitaxial layer: Part I. geometry and crystallography. *Phys. Stat. Sol.* **198**, 599–613 (1996)

49. Romanov, A.E., Pompe, W., Beltz, G., Speck, J.S., Mathis, S.: Threading dislocation reduction in strained layers. *J. Appl. Phys.* **85**(1), 182–192 (1999)
50. Speck, J.S., Brewer, M.A., Beltz, G., Romanov, A.E., Pompe, W.: Scaling laws for the reduction of threading dislocation densities in homogenous buffer layer. *J. Appl. Phys.* **80**(7), 3808–3816 (1996)
51. Mathis, S.K., Romanov, A.E., Chen, L.F., Beltz, G., Pompe, W., Speck, J.S.: Modeling of threading dislocation reduction in growing GaN layers. *Phys. Stat. Sol.* **179**, 125–145 (2000)
52. Haerberlen, M., Zhu, D., McAleese, C., Kappers, M.J., Humphreys, C.J.: Dislocation reduction in MOVPE grown GaN layers on (111) Si using SiNx and AlGaN layers. *J. Phys Conf. Ser.* **209**, 012017 (2010)
53. Yamamoto, A., Sugita, K., Horie, M., Ohmura, Y., Islam, Hashimoto, A.: Mg-doping and n + -p junction formation in MOVPE-grown $\text{In}_x\text{Ga}_{1-x}\text{N}$ ($x \sim 0.4$). 33rd IEEE Photovoltaic Specialist Conference, San Diego (2008)
54. Liou, B.T., Lin, C.Y., Yen, S.H., Kuo, Y.K.: First-principles calculation for bowing parameter of wurtzite $\text{In}_x\text{Ga}_{1-x}\text{N}$. *Opt. Commun.* **249**, 217 (2005)
55. Detchprohm, T., Hiramatsu, K., Itoh, K., Akasaki, I.: Relaxation process of the thermal strain in the GaN/ α -Al₂O₃ heterostructure and determination of the intrinsic lattice constants of GaN free from the strain. *Jpn. J. Appl. Phys.* **31**, L1454–L1456 (1992)
56. Paszkowicz, W.: X-ray powder diffraction data for indium nitride. *Powder Diff.* **14**, 258 (1999)